International Journal of Nanomedicine

Dovepress
open access to scientific and medical research

Open Access Full Text Article

ORIGINAL RESEARCH

Enhanced antitumor efficacy of doxorubicin-encapsulated halloysite nanotubes

This article was published in the following Dove Press journal:
International Journal of Nanomedicine

Kai Li[1,*]
Yongxing Zhang[2,*]
Mengting Chen[1]
Yangyang Hu[1]
Weiliang Jiang[1]
Li Zhou[1]
Sisi Li[1]
Min Xu[1]
Qinghua Zhao[2]
Rong Wan[1]

[1]Department of Gastroenterology, Shanghai First People's Hospital, School of Medicine, Shanghai Jiao Tong University, Shanghai, People's Republic of China; [2]Department of Orthopaedics, Shanghai First People's Hospital, School of Medicine, Shanghai Jiao Tong University, Shanghai, People's Republic of China

*These authors contributed equally to this work

Abstract: To improve the antitumor efficacy of doxorubicin (DOX) and provide novel clinical treatment of gastric cancer, halloysite nanotubes (HNTs) loaded with DOX were encapsulated by soybean phospholipid (LIP) and the formed HNTs/DOX/LIP was systematically characterized via different techniques. The in vitro anticancer activity of HNTs/DOX/LIP was examined using an MTT assay. The antitumor efficacy and biocompatibility were monitored by measuring the tumor volume and assessing the blood routine and serum biochemistry using an ectopic implantation cancer model. The results show that when the concentration of HNTs was 3 mg/mL and the concentration of DOX was 1 mg/mL the optimal DOX loading efficiency was as high as 22.01%±0.43%. In vitro drug release behavior study demonstrated that HNTs/DOX/LIP shows a pH-responsive release property with fast drug release under acidic conditions (pH =5.4). MTT assays and in vivo experimental results revealed that HNTs/DOX/LIP exhibits a significantly higher inhibitory efficacy on the growth of mouse gastric cancer cells than free DOX at the same drug concentration. In addition, the life span of tumor-bearing mice in the HNTs/DOX/LIP-treated group was obviously prolonged compared with the control groups. Moreover, HNTs/DOX/LIP possessed excellent hemocompatibility as shown in the blood and histology studies. These findings indicated that the formed HNTs/DOX/LIP possesses higher antitumor efficacy and may be used as a targeted delivery nanoplatform for targeting therapy of different types of cancer cells.

Keywords: HNTs, DOX, gastric cancer, drug carrier

Introduction

Gastric cancer, the fourth most malignant tumor, has an annual death toll as high as 738,000, second only to lung cancer.[1] Also, it had the second highest incidence (36.21/10 million) and the third highest mortality rate (25.88/10 million) in the People's Republic of China in the 2012 statistics.[2] Until now, radical surgery remains the only means to cure gastric cancer at its early clinical stage. However, more than half of patients miss the best time for surgery due to unobservable clinical symptoms of early gastric cancer. With the standardization of surgical options and the development of new anticancer drugs, considerable progress has been made in the treatment of gastric cancer, however, mortality is still high.

Compared with the best supportive treatment, chemotherapy provides patients prolonged life and an improved quality of life with progressed gastric cancer.[3,4] However, there are a series of obvious defects in chemotherapy. First, antitumor drugs in the body do not show any specificity to the tumor site, and thus has systemic toxic side effects.[5] Second, multi-administration is required for most of the drugs to maintain high efficiency to kill cancer cells and minimize side effects. However, this kind of therapy significantly increases the cost and is a waste of medical resources.

Correspondence: Rong Wan
Department of Gastroenterology, Shanghai First People's Hospital, School of Medicine, Shanghai Jiao Tong University, 100 Haining Road, Shanghai 200080, People's Republic of China
Tel +86 21 3612 3151
Email rongwan1970@126.com

Qinghua Zhao
Department of Orthopaedics, Shanghai First People's Hospital, School of Medicine, Shanghai Jiao Tong University, 100 Haining Road, Shanghai 200080, People's Republic of China
Tel +86 21 3779 8591
Email sawboneszhao@163.com

submit your manuscript | www.dovepress.com
Dovepress
http://dx.doi.org/10.2147/IJN.S143928

Third, the effect of chemotherapy was significantly limited by the relatively short retention time of small molecular drugs (such as doxorubicin [DOX]) in highly permeable cancerous tissue.[6] Moreover, repeated low-dose chemotherapy can easily lead to tumor multidrug resistance.[7,8]

Nanoparticles, typically with a particle size ranging from 0.1 to 100 nm, have high surface activity that confer a series of unique advantages. Most of the nanoparticles can pass through the cell membrane and are considered good carriers for drug delivery.[9] Additionally, nanoparticles-based drug delivery systems could significantly increase the uptake of antitumor drugs in the tumor site through active or passive targeting effect. Therefore, the development of nanotechnology has made a huge contribution for more efficient drug carriers with less side effects.[10,11] Halloysite, comprising aluminum silicate salt natural nanotubes, is often used as fireproof material and anticorrosive coating additive[12,13] due to its special properties, such as larger specific surface area, non-toxicity, good thermal stability, and low cost.[14,15] Recent studies have confirmed that the use of halloysite nanotubes (HNTs) could prevent rapid enzymatic degradation of drugs in the human body, thus effectively delaying drug release. For example, Viseras[16] reported the use of HNTs as carriers for targeted large intestine delivery of 5-amino salicylic acid with controlled release properties. Also, HNTs can be used to encapsulate drugs and effectively retard their release by preventing rapid degradation in vivo. Therefore, they received much attention and have gradually become hot spots in the field of nanomedicine.

Since the end of the 19th century, DOX became a milestone in cancer treatment. DOX is a small molecule anticancer drug and can be easily absorbed by cancer cells, which weakens the infiltration and therapeutic effect of this drug.[17] With highly effective cytotoxicity, a wide antitumor spectrum, and precise curative effect, DOX is widely accepted as the most powerful clinical antitumor drug. In combination with other drugs, DOX increases the long-term survival rate of breast cancer patients by over 70%. However, recent years have witnessed some serious side effects in the clinical application of DOX, such as reactive oxygen species overproduction, lipid peroxidation, DNA damage, accumulation of tumor suppressor protein, and cardiac toxicity.[18–20] Thus, the development of various drug delivery systems with lesser side effects still remains a great challenge.[21]

In order to gain more ideal efficacy and less toxic side effects, researchers have developed a variety of DOX delivery vectors based on different nanomaterials, including dendrimers,[22,23] micelles,[24] liposomes,[25] carbon nanotubes, graphene,[26,27] laponite nanodisks,[28] and inorganic nanoparticles.[29] In the present study, HNTs loaded with the antitumor drug DOX were encapsulated by soybean phospholipid (LIP) to generate HNTs/DOX/LIP complexes. X-ray diffraction (XRD) and ultraviolet–visible (UV-vis) technologies were used to qualitatively confirm the feasibility of DOX-loaded HNTs. Transmission electron microscopy (TEM) and field-emission scanning electron microscopy (FESEM) were used to measure the morphological changes of HNTs after phospholipid coating. Thermal gravimetric analysis (TGA) was employed to qualitatively verify the coated phospholipid. MTT assays were performed to evaluate the cytotoxicity of HNTs/DOX/LIP in vitro, and a nude mice xenograft tumor model was used to evaluate their antitumor effects and in vivo distribution. These results reported the use of HNTs as antitumor drug carriers and highlighted its excellent antitumor activity, desired biocompatibility, and less side effect. Therefore, it lay the foundation for the future development of effective, biocompatible, and enhanced antitumor drugs and provides a new method for clinical oncology therapy.

Materials

HNTs were supplied by Zhejiang Institute of Geologic and Mineral Resources (Hangzhou, Zhejiang, People's Republic of China). DOX (in a hydrochloride form; unless otherwise stated, the term DOX indicates DOX·HCl) was purchased from Beijing Huafeng Pharmaceutical Co, Ltd (People's Republic of China). Mouse forestomach carcinoma (MFC) cells were obtained from the Institute of Biochemistry and Cell Biology (the Chinese Academy of Sciences, Shanghai, People's Republic of China). Fetal bovine serum, Roswell Park Memorial Institute-1640 (RPMI-1640), penicillin, and streptomycin were obtained from Hangzhou Jinuo Biomedical Technology Co, Ltd (Hangzhou, People's Republic of China). All other chemicals were purchased from Sigma-Aldrich Co (St Louis, MO, USA). Water used in all the experiments was purified by a water purification system (Milli-Q Plus 185; EMD Millipore, Billerica, MA, USA).

Loading of DOX

The HNTs/DOX complexes were generated by mixing HNT aqueous solution (3 mg/mL, 10 mL) with DOX aqueous solution (1 mg/mL, 10 mL) under magnetic stirring for 24 hours to facilitate interactions between HNTs and DOX. The complexes were rinsed three times with water and dried in air, and finally stored under dark and room temperature conditions. The optimized loading efficiency of HNTs/DOX was 22.01%±0.43%.

Soybean phospholipid modification

An aliquot of 100 mg HNTs/DOX was dispersed in anhydrous ethanol (2 mg/mL) and subjected to ultrasonic dispersion (500 W) for 30 minutes, followed by mixing with soybean phospholipid (10 mg/mL) and ultrasonic dispersion (100 W) for an additional 5 minutes. The ethanol dispersion liquid was transferred to a 500-mL round bottom flask and placed on a steamed rotary evaporator (60°C, 90 rotations/min) to evaporate ethanol. After cooling, 100 mL of saline was added to the above mixture, and then it was subjected to ultrasonic dispersion for 30 minutes.

Characterization

For TGA analysis, different aspects of LIP, DOX, HNTs, HNTs/DOX, and HNTs/DOX/LIP samples were examined in aluminum pots. The temperature was increased at the rate of 10°C/min under nitrogen protection (90 mL/min) with temperatures ranging from 25°C to 1,000°C. FESEM was performed using an FEI Magellan 400 field-emission microscope (Thermo Fisher Scientific, Waltham, MA, USA). TEM was carried out on a JEOL 2010F analytical electron microscope (JEOL, Tokyo, Japan) under an acceleration voltage of 200 kV. XRD was performed using a Rigaku D/max 2550 PC (Rigaku, Tokyo, Japan) with Cu Kα radiation. Fourier-transform infrared spectroscopy (FTIR) and UV-vis spectrometry were performed using a Nicolet Nexus 670 FTIR (650–4,000 cm^{-1}; GMI Inc., Ramsey, MN, USA) and a Lambda 25 spectrometer (250–700 nm; GMI Inc.), respectively.

In vitro release experiment

The HNTs/DOX/LIP samples were dissolved in sodium acetate buffer (pH =5.4) and phosphate-buffered saline (PBS, pH =7.4) with the same concentration of 1 mg/mL, respectively. Subsequently, 1 mL of the mixture was transferred to dialysis bags, placed in a reaction flask containing 9 mL of the corresponding buffer solution, and transferred to a reaction bottle, followed by incubation at 37°C to hatch. At each predetermined time point, 1 mL of the liquid outside the dialysis bag was collected, and 1 mL of corresponding buffer solution was supplemented. The concentration of released DOX was determined using a standard curve. The cumulative release of DOX at different time points was calculated, and the release kinetics of the drug were analyzed.

Cell cultures and in vitro tumor therapy of HNTs/DOX/LIP complexes

MFC mouse gastric cancer cells were used to verify the antitumor effects of HNTs/DOX/LIP by MTT viability assay. Briefly, cells were cultivated, collected, and seeded onto a 96-well plate at a density of 8,000 cells/well with 100 mL RPMI-1640 medium. After overnight incubation, the drugs with different concentrations were added and removed after 24 hours incubation. MTT was added to the solution (10 μL/well), and the cells were incubated for another 4 hours. Subsequently, DMSO (100 μL/well) was added, and the cells were incubated at room temperature with shaking for 20 minutes. An MK3 reader (Thermo Fisher Scientific) was used to read the absorbance at 570 nm and evaluate the inhibitory effect of HNTs/DOX/LIP on the gastric cancer cells.

Tumor models and in vivo tumor therapy of HNTs/DOX/LIP complexes

All animal experimental procedures were performed under protocols approved by the Shanghai Jiao Tong University Laboratory Animal Center (Shanghai, People's Republic of China). Male nude mice (4–6 weeks old) were obtained from Shanghai SLAC Laboratory Animal Co Ltd (Shanghai, People's Republic of China). For tumor model preparation, the back of each nude mouse (n=3×6) was subcutaneously injected with 2×10^6 MFC mouse gastric cancer cells in 200 μL serum-free RPMI-1640 medium.

When the tumor reached a volume of 0.5 cm^3 (~2 weeks), the nude mice were treated with 100 μL of HNTs/DOX/LIP (1.2 mg/mL DOX), free DOX (1.2 mg/mL), or saline (control) (n=6 for each group). The relative tumor volume (V/V_0, V_0=0.5 cm^3), body weight, tumor appearance, and survival time of each nude mice were recorded at different time points.

To determine the long-term fate of HNTs in vivo, 4–6 weeks old healthy Kunming mice (Shanghai SLAC Laboratory Animal Co Ltd) were used. Fifteen mice were caudal vein injected with 100 μL of HNTs/DOX/LIP solution and euthanized at 1, 3, 7, 14, and 21 days postinjection (n=3 for each time point), respectively. The different organs, including liver, heart, lungs, spleen, and kidney, were harvested, weighed, and then digested overnight using aqua regia solution. The silicon uptake in different organs was subsequently quantified using Leeman Prodigy inductively coupled plasma optical emission spectroscopy (ICP-OES; Hudson, NY, USA).

Blood examination

Twenty 4–6 weeks old healthy Kunming mice were caudal vein treated with 100 μL of saline (control) and HNTs/DOX/LIP (n=2×10). On day 7 and 14 postinjection (five mice for each time point), each mouse was anesthetized and punctured in the heart to collect blood. Routine blood tests, including

hemoglobin (Hb), white blood cells (WBC), and platelets (PLT), were recorded using a Sysmex XS-800i automated hematology analyzer (Sysmex Corporation, Kobe, Japan). Subsequently, the blood was centrifuged, and the supernatant was collected to test the serum biochemical activity, such as alanine aminotransferase (ALT), aspartate aminotransferase (AST), total bilirubin (TB), serum creatinine (SCR), and blood urea nitrogen (BUN), using a Beckman Coulter UniCel DxC 800 automatic biochemical analyzer (Beckman Coulter Inc, Brea, CA, USA).

Histology examination

To evaluate the antitumor efficacy and biosafety of HNTs/DOX/LIP complexes in vivo, histological analyses were performed. Three tumor-bearing mice were caudal vein injected with 100 µL of HNTs/DOX/LIP (1.2 mg/mL DOX), free DOX (1.2 mg/mL), or saline. Each mouse was euthanized on day 14 postinjection, and then the tumors were harvested for H&E staining. To evaluate the antitumor efficacy, eight tumor-bearing mice were caudal vein injected with 100 µL of the HNTs/DOX/LIP complexes (1.2 mg/mL DOX), free DOX (1.2 mg/mL), or saline (control group) (n=3×2). The mice were euthanized at 7 and 14 days after treatment (one mouse for each time point), and different tumor sections were stained using an antibody against the endothelial marker, CD31 (BD Biosciences, San Jose, CA, USA) according to the manufacturer's instructions.

To assess biosafety, two healthy Kunming mice were caudal vein injected with 100 µL of HNTs/DOX/LIP (1.2 mg/mL DOX) or saline, respectively. They were euthanized at 45 days after treatment. Subsequently, the different organs, including liver, heart, lungs, spleen, and kidney, were harvested, fixed with 10% neutral-buffered formalin, embedded in paraffin, sectioned into 8-µm thick slices, stained with H&E, and examined using an inverted phase contrast microscope (Leica DM IL LED; Leica Microsystems, Wetzlar, Germany).

Statistical analysis

Statistical analysis using one-way analysis of variance was performed to evaluate the significance of the experimental data, and 0.05 was selected as the significance level. Data were indicated with (*) for $p<0.05$, (**) for $p<0.01$, and (***) for $p<0.001$.

Results and discussion

To apply HNTs/DOX for the treatment of cancer, we first studied the drug loading efficiency of the formed nanocomplexes. The load efficiency curves for different concentrations of HNTs and DOX were plotted according to the results of the experiment. As shown in Figure 1A, the drug loading efficiency gradually increased with increasing HNT concentration, because the high concentration of HNTs facilitates the absorption of DOX molecules both in the lumen and on the surface. However, with the concentration beyond a certain range, HNTs in the solution might aggregate, which is not conducive to the adsorption of DOX. The optimized drug loading efficiency was 22.01%±0.43% when the concentration of HNTs was 3 mg/mL. Therefore, we selected HNTs carrying DOX at concentrations of 3 or 1 mg/mL as the best drug loading conditions. According to a previous study, improving drug loading efficiency can significantly

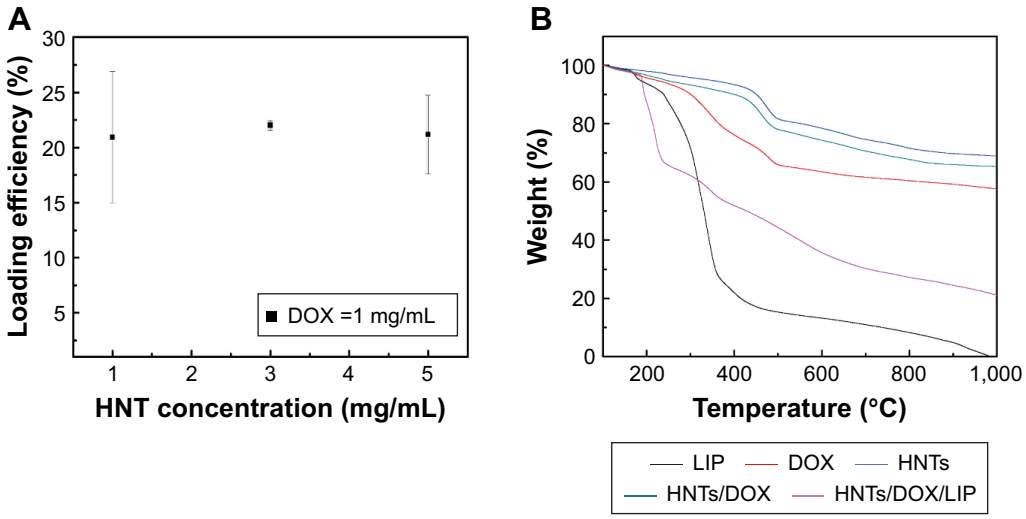

Figure 1 (**A**) Loading efficiency of DOX in different HNT concentrations. (**B**) TGA curve of LIP, DOX, HNTs, HNTs/DOX, and HNTs/DOX/LIP.
Abbreviations: DOX, doxorubicin; HNT, halloysite nanotube; LIP, soybean phospholipid; TGA, thermal gravimetric analysis.

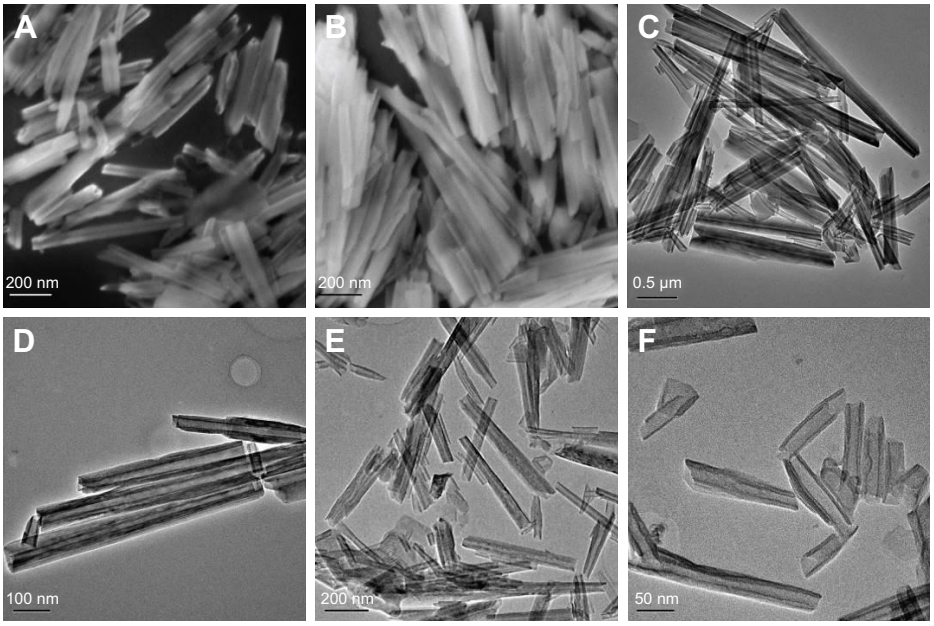

Figure 2 FESEM images of (**A**) HNTs and (**B**) HNTs–LIP. TEM images of (**C**, **D**) HNTs and (**E**, **F**) HNTs/DOX/LIP.
Abbreviations: DOX, doxorubicin; FESEM, field-emission scanning electron microscopy; HNTs, halloysite nanotubes; LIP, soybean phospholipid; TEM, transmission electron microscopy.

reduce drug dose,[30] thereby avoiding unnecessary wastage of drugs and reducing the toxicity and side effects.

The inner and outer sides of the structures of HNTs are different: the outside layer is negatively charged and the inner layer is positively charged. This characteristic makes it easy to combine HNTs with sodium, chlorine, and other charged ions in the blood, potentially forming a thrombus and blocking the blood vessel. Therefore, after DOX loading, we used soybean phospholipid modification to package and isolate the complex from direct contact with the sodium and chloride ions. TGA was used to verify the success of the package. As shown in Figure 1B, the weight loss of HNTs/DOX and HNTs was only 5.44% and 8.57% at 360°C, respectively, whereas the HNTs/DOX/LIP weight loss was 44.85%. Thus, weight loss of ~36.28% represents modified LIP on the surface. Before and after LIP modification, we used FESEM and TEM to compare the morphology changes of the HNTs. As shown in Figure 2, their morphology showed minor changes. We also used XRD to compare the crystal structure of HNTs and HNTs/DOX/LIP. As shown in Figure 3A, the XRD patterns of HNTs and HNTs/DOX/LIP are the same. The attenuated total reflectance FTIR of HNTs/DOX/LIP showed absorption peaks of $-CH_2$ (2,924 cm^{-1}), C=O (2,854 cm^{-1}), C=C (1,736 cm^{-1}), P–O–C (1,225 cm^{-1}), and C–O–C (1,050 cm^{-1}) (Figure 3B), which belong to the characteristic structure of soybean phospholipids,[31] further confirming the success of the surface LIP modification. The hydrodynamic size of the HNTs–LIP measured by dynamic

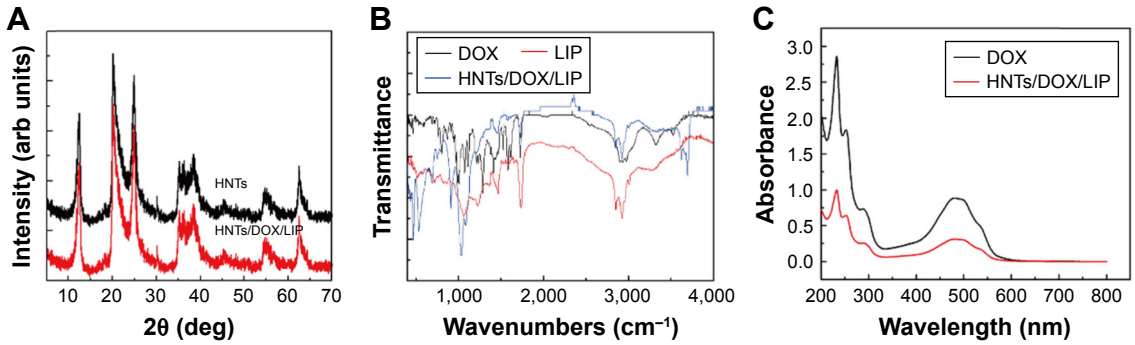

Figure 3 (**A**) XRD of HNTs and HNTs/DOX/LIP. (**B**) ATR-FTIR of DOX, LIP, and HNTs/DOX/LIP. (**C**) UV-vis of DOX and HNTs/DOX/LIP.
Abbreviations: arb, arbitrary; ATR, attenuated total reflectance; DOX, doxorubicin; FTIR, Fourier-transform infrared spectroscopy; HNTs, halloysite nanotubes; LIP, soybean phospholipid; UV-vis, ultraviolet–visible; XRD, X-ray diffraction.

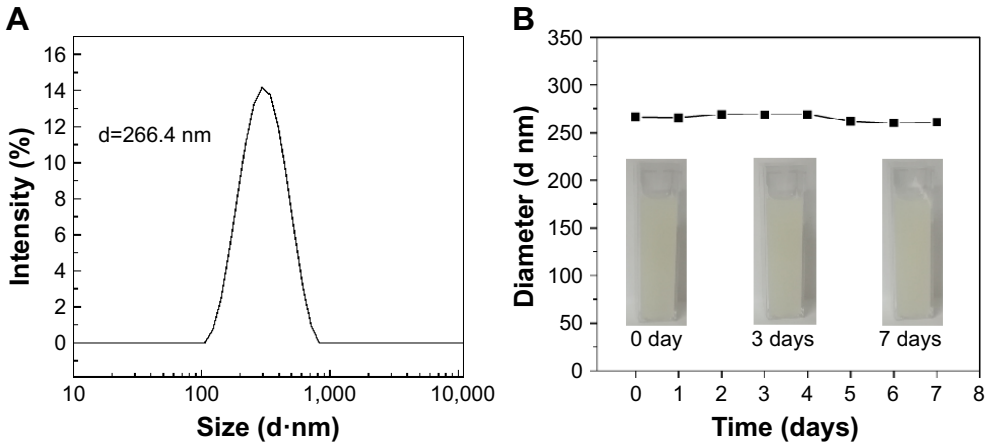

Figure 4 (**A**) The hydrodynamic size distribution of HNTs–LIP dispersed in water. (**B**) Diameter changes of HNTs–LIP dispersed in PBS solvents at varied time points. Insets are the corresponding digital images.
Abbreviations: d, diameter; HNTs, halloysite nanotubes; LIP, soybean phospholipid; PBS, phosphate-buffered saline.

light scattering was 266.4±0.9 nm (Figure 4A). The stability of the HNTs–LIP is an important issue for their biomedical applications. As shown in Figure 4B, the diameter of HNTs–LIP dispersed in PBS solvents does not have any appreciable changes at varied time points, suggesting that the HNTs–LIP is stable in PBS solvents.

We further used UV-vis to verify the successful loading of DOX. As shown in Figure 3C, HNTs maintained a regular tubular structure, suggesting that the load does not change the morphology of HNTs. Also, both DOX and HNTs/DOX/LIP exhibited characteristic absorption at 480 nm, further confirming the successful loading of DOX.

With their unique physical and chemical properties, HNTs have a distinct advantage in molecular loading and have been widely used in the field as drug carriers. This application is primarily shown in two aspects: on one hand, the negatively charged surface of HNTs (−16.5±1.2 mV) can easily combine with the positively charged molecules; on the other hand, HNTs have a special nanotubular structure and a large specific surface area. Therefore, these molecules have strong adsorption capacities.[32] However, there is currently no relevant research on the load mechanism of DOX for HNTs. In this work, we speculated that this mechanism might be related to the two reasons stated below. First, DOX, which has a positively charged surface, can combine with HNTs through charge attractions. Moreover, the larger specific surface area of HNTs has a strong adsorption capacity for DOX. The diffraction peaks of DOX were clearly detected from the XRD spectra of HNTs/DOX/LIP, which verified the successful loading of DOX onto the HNT.

The application of DOX is largely limited by its side effects. We conceived that the drug can be selectively released at the tumor site by drug carrier load, which avoids the exposure of the drug in normal tissue, thereby reducing the damage to normal tissue. As shown in Figure 5A, the release rate of HNTs/DOX/LIP in the weak acid environment

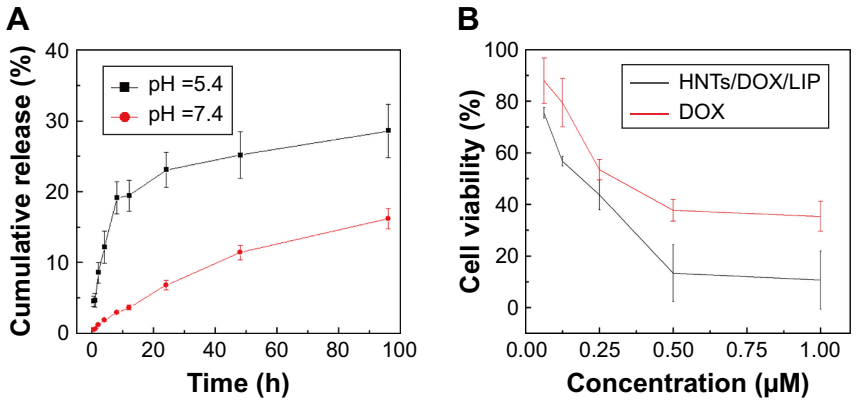

Figure 5 (**A**) Cumulative release curve of DOX from HNTs/DOX/LIP in different pH values (mean ± SD, n=6). (**B**) Cell viability assay of MFC mice gastric cancer cells after treatment with DOX or HNTs/DOX/LIP for 24 hours (mean ± SD, n=6).
Abbreviations: DOX, doxorubicin; HNTs, halloysite nanotubes; LIP, soybean phospholipid; MFC, mouse forestomach carcinoma.

(pH =5.4) is faster than that in the physiological environment (pH =7.4). In a weak acid environment of pH =5.4, the release amount of DOX is closer to linear growth, and the cumulative release amount of DOX/HNTs can reach nearly 30% after 4 days. In general, with the rapid growth of tumor cells, there may be a shortage in the supply of nutrient and oxygen. Also, the pH value of the tumor microenvironment is lower than that in the normal position, facilitating the distribution of DOX at the tumor site. Thus, DOX loading onto HNTs reduces the damage to normal tissue cells and more effectively inhibits the proliferation of cancer cells. The data shown in Figure 5A suggest that the release rate of DOX from HNTs/DOX/LIP is closely related to the pH value of the microenvironment. This result primarily means that the acidic environment facilitates DOX release as the water-soluble hydrochloride (DOX·HCl), which is unstable in neutral environments (pH =7.4) and tends to become hydrophobic drug molecules combining with carrier molecules.[33] This is beneficial for drug release at the tumor site and increases the drug concentration and prolongs the action time at the tumor site. Simultaneously, the drug release amount is effectively reduced in the normal tissue, thereby greatly reducing the side effects.

To verify the effect of the HNTs/DOX/LIP drug delivery system for the treatment of cancer, we evaluated the inhibitory effect of HNTs/DOX/LIP on gastric cancer cells using the MTT colorimetric method. As shown in Figure 5B, the inhibitory effect of HNTs/DOX/LIP and DOX on cancer cells was enhanced with increasing DOX concentration. At the same DOX concentration, the inhibition of HNTs/DOX/LIP on the cells was significantly better than that of DOX, suggesting that HNTs/DOX/LIP more effectively inhibits the proliferation of cancer cells. The aluminum uptake in MFC mice gastric cancer cells was, respectively, five and eight times higher at the HNTs–LIP concentration of 50 and 100 ppm, compared with the control (Figure 6).

We used the MFC mice gastric cancer mouse model to study the effects of HNTs/DOX/LIP in vivo. As shown in Figure 7, the sizes of the tumor were initially the same in all three groups. After 14 days of feeding, the tumor sizes in the DOX and saline groups were 3.964 and 5.578 cm^3, respectively. Because of the large size, insufficient blood supply led to distal necrosis of the tumor. In contrast, tumor growth was obviously slow in the treatment group, and the volume was only 1.863 cm^3. As shown in Figure 8A, the tumor size varied from large to small in the following order: saline group > DOX group > HNTs/DOX/LIP group. These results indicated that the effect of HNTs/DOX/LIP was better

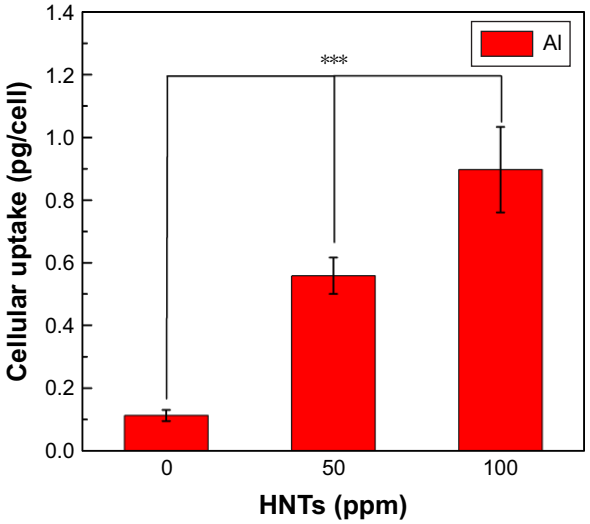

Figure 6 Cellular uptake of Al in MFC mice gastric cancer cells treated with HNTs/DOX/LIP at different concentrations for 24 hours.
Note: ***$p<0.001$.
Abbreviations: DOX, doxorubicin; HNTs, halloysite nanotubes; LIP, soybean phospholipid; MFC, mouse forestomach carcinoma.

than that of DOX alone. We calculated the survival time and long-term survival rate of each group to evaluate the antitumor effect of the drug. As shown in Figure 8B, in the saline group, rapid proliferation and metastasis of tumor cells led to the death of the first mouse at 15 days after treatment, and all of the mice died within 26 days. In the DOX group, the death of the first nude mouse was observed at 13 days after treatment. This finding might reflect the toxicity of high-dose DOX or individual animal differences, and 16.67% nude mice survival was observed at the end of the observation period. This result indicates the excellent antitumor effect of DOX. In the HNTs/DOX/LIP group, the first nude mouse died after 21 days, showing a longer survival time than the mice in the DOX (13 days) and saline (15 days) groups. In addition, 40 days after the administration of HNTs/DOX/LIP, 50% of the experimental animals survived, indicating that the survival time was significantly prolonged. These results further confirm that HNTs/DOX/LIP can improve the antitumor effect of DOX.

In addition, we also used immunohistochemistry for the endothelial cell tumor marker CD31 to evaluate the antitumor effect of HNTs/DOX/LIP complexes. CD31, also known as PLT endothelial cell adhesion molecule, is a marker of microvasculature. It is primarily expressed and widely distributed in vascular cells, and closely related to the formation of vasculature. As a specific indictor of vascular endothelial cells, CD31 can be used for the quantitative assessment of the role of the angiogenesis factor in angiogenesis.[34] Thus, in the present study, we considered the tumor expression

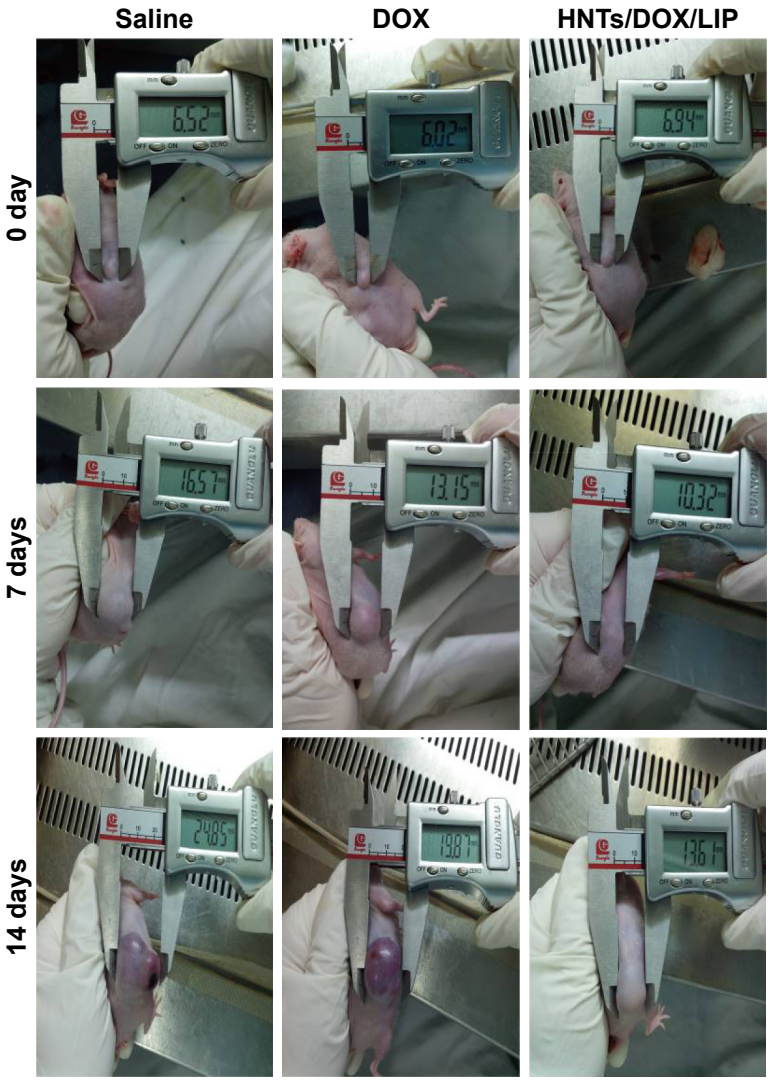

Figure 7 Representative photographs of MFC mice gastric cancer-bearing mice after various treatments at day 0, 7, and 14.
Abbreviations: DOX, doxorubicin; HNTs, halloysite nanotubes; LIP, soybean phospholipid; MFC, mouse forestomach carcinoma.

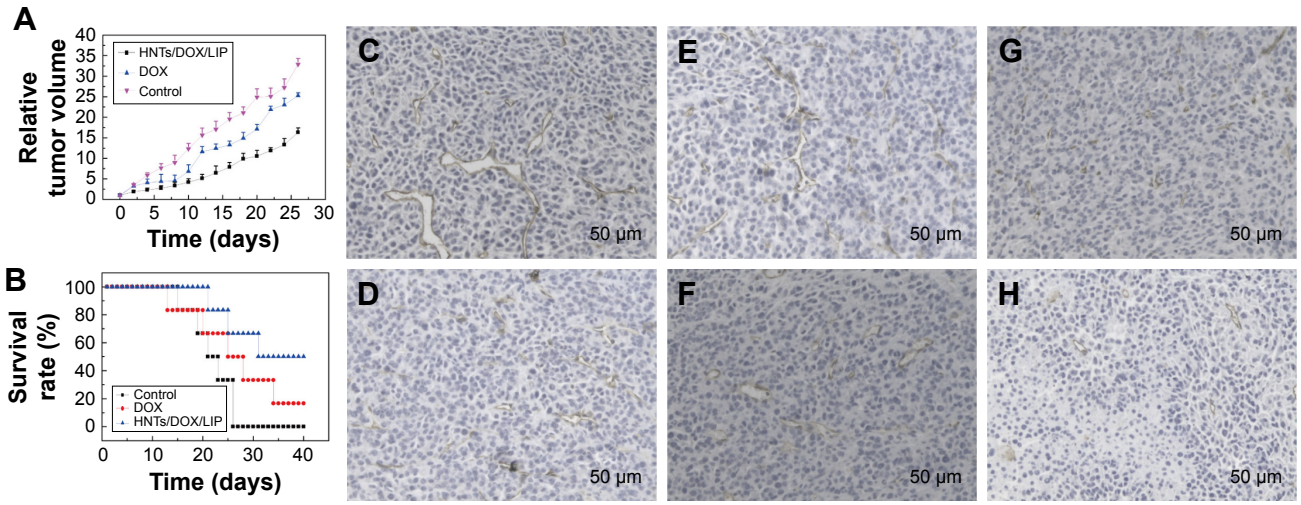

Figure 8 The relative tumor volumes were normalized according to their initial sizes (mean ± SD, n=6). The growth of MFC mice gastric cancer xenografted tumors (**A**) and the survival rate of mice (**B**) after various treatments. Immunohistochemical staining for CD31 expression of tumor sections in mice after 7 (**C**, **E**, **G**) and 14 days (**D**, **F**, **H**) treatment with saline (**C**, **D**), free DOX (**E**, **F**), and HNTs/DOX/LIP (**G**, **H**). Magnification 200×.
Abbreviations: DOX, doxorubicin; HNTs, halloysite nanotubes; LIP, soybean phospholipid.

of CD31 as a judgment index of tumor growth, metastasis, and recurrence.[35] CD31-positive microvessels were dyed brown, and the more densely brown a single high-powered field is, the higher the CD31 expresses, indicating exuberant angiogenesis, such as faster tumor growth rate and worsening drug inhibition effect. As shown in Figure 8C, E, and G, at 7 days after treatment, compared with the saline group, CD31 expression decreased in the DOX and HNTs/DOX/LIP groups, and the HNTs/DOX/LIP showed a more obvious reduction, suggesting that DOX and HNTs/DOX/LIP inhibit the formation of tumor angiogenesis. This effect primarily indicated the fact that DOX blocks DNA in the S phase of cancer cell division.[36] However, at 14 days after drug application (Figure 8D, F, and H), the CD31 expression in the saline and DOX groups was significantly increased but obviously decreased in the HNTs/DOX/LIP group. The positive expression of CD31 in the DOX group indicates the rapid metabolism of DOX. Further reduction of CD31 expression in the HNTs/DOX/LIP group proved that the metabolism of HNTs/DOX/LIP was slower than that of DOX and therefore the effect may be more durable. The stronger antitumor effect might result from DOX packed in HNTs, which enhanced the uptake of DOX in cancer cells. In addition, the tumor acidic environment increased the release of DOX from HNTs/DOX after intravenous injection, and further enhanced the antitumor effects of this drug. Moreover, the antitumor effect of the HNTs/DOX/LIP complex was enhanced by passive targeting, enhanced DOX uptake, and accumulation in tumor site through the enhanced permeability and retention (EPR) effects. In contrast, DOX was evenly distributed throughout the entire body after intravenous injection and rapidly metabolized through the excretory system. Although DOX was only partially taken in by cancer cells, it may also be execrated by P-glycoprotein and other DOX-sensitive molecular protein immediately; therefore, the antitumor effect of free DOX decreased greatly.[36,37]

For the HNTs/DOX/LIP complex, it is important to explore the fate of HNTs after intravenous injection. We detected the distribution of HNTs after intravenous injection of HNTs/DOX/LIP. We used ICP-OES to quantitatively detect the concentrations of silicon ions in major organs (heart, liver, spleen, lungs, and kidney) at different times (1, 3, 7, 14, and 21 days) to evaluate the distribution of HNTs (Figure 9A). It was obvious that the heart, lungs, and kidney all took in small amounts of silicon at the time point examined. In contrast, the liver and spleen, belonging to the reticuloendothelial system, took up more silicon: 12.31 μg/g (day 1), 15.27 μg/g (day 3), 28.74 μg/g (day 7), 13.40 μg/g (day 14), 5.41 μg/g (day 21); and 10.61 μg/g (day 1), 12.26 μg/g (day 3), 23.47 μg/g (day 7), 1.235 μg/g (day 14), 4.54 μg/g (day 21), respectively. Different amounts of silicon uptake showed that the HNTs/DOX/LIP complex could be transferred from the tumor site to the reticuloendothelial system through the blood or lymph circulation.[38] The organ

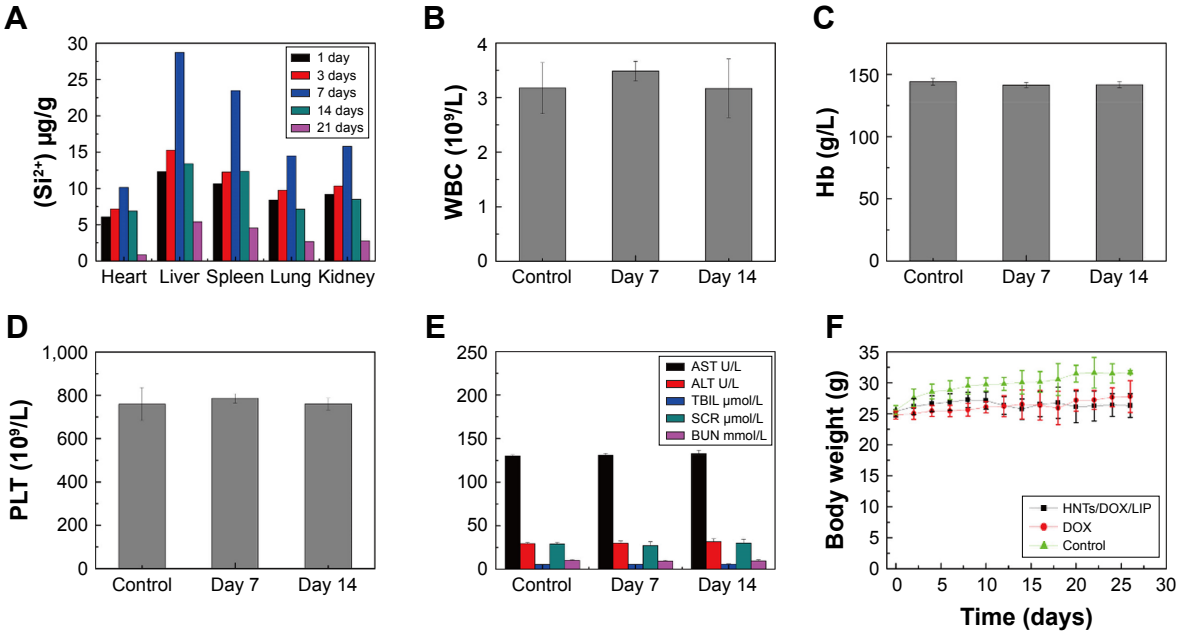

Figure 9 (**A**) In vivo biodistribution of HNTs after 1, 3, 7, 14, and 21 days caudal vein injected with HNTs/DOX/LIP complexes (mean ± SD, n=3). (**B**–**D**) Hematology data and (**E**) blood biochemistry of mice at days 7 and 14 posttreatment with saline (control) and HNTs/DOX/LIP. (**F**) Body weight of MFC mice gastric cancer-bearing mice after various treatments (mean ± SD, n=3).

Abbreviations: ALT, alanine aminotransferase; AST, aspartate aminotransferase; BUN, blood urea nitrogen; DOX, doxorubicin; Hb, hemoglobin; HNTs, halloysite nanotubes; LIP, soybean phospholipid; MFC, mouse forestomach carcinoma; PLT, platelet; SCR, serum creatinine; TBIL, total bilirubin; WBC, white blood cells.

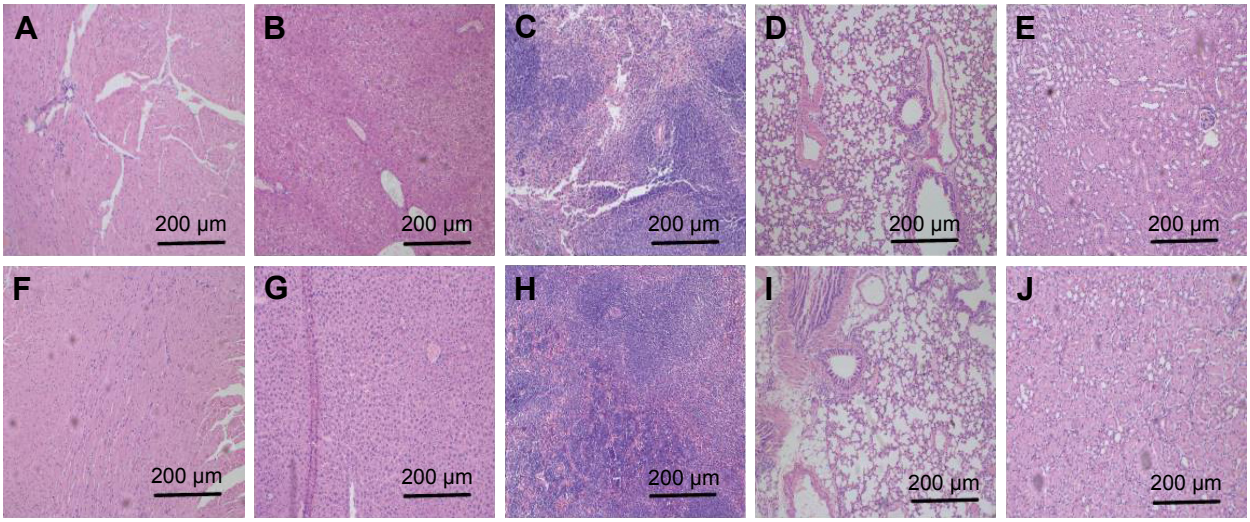

Figure 10 H&E stained tissue sections of major organs, including the heart (**A** and **F**), liver (**B** and **G**), spleen (**C** and **H**), lung (**D** and **I**), and kidney (**E** and **J**) from mice caudal vein injected with saline (**A–E**) or HNTs/DOX/LIP complexes (**F–J**) at day 14.
Abbreviations: DOX, doxorubicin; HNTs, halloysite nanotubes.

silicon content at 7 days after treatment was significantly reduced, suggesting that HNTs were cleared through the reticuloendothelial system, blood, and lymph circulation.

To further illustrate the advantages of HNTs as antitumor drug carriers, we also examined the in vivo biological safety of HNTs/DOX/LIP complexes. In these experiments, we studied the biocompatibility of HNTs through the detection of the blood routine and biochemistry of the experimental animals. After treatment for 7 and 14 days, the mice were anesthetized, and heart puncture was performed to obtain blood samples. As shown in Figure 9B–E, at both time points, the blood routine (including Hb, WBC, and PLT) and blood biochemical activity (including AST, ALT, TB, SCR, and BUN) in the three groups showed no significant difference. Also, the morphological observation of the main organs and tissues at 7 and 14 days after treatment, as shown in Figure 9F, showed no obvious inflammation, cell infiltration, necrosis, or other significant differences between the HNTs/DOX group and the control group. These results indicate that after administering saline and HNTs/DOX/LIP complexes, Kunming rats remained healthy. Therefore, we concluded that there is no obvious systemic toxicity when HNTs/DOX/LIP complexes serve as an anticancer drug delivery system.

Moreover, we also monitored the body weight changes of tumor-bearing nude mice. As shown in Figure 10A–E (7th day) and F–J (14th day), the animals' weight showed no significant difference before and after treatment in the DOX and HNTs/DOX/LIP groups. However, the average weight of the mice in the saline group was significantly increased after the administration compared with that before treatment. This is because the tumor growth of the nude mice in the saline group was faster, which increased weight gain far more than weight loss resulting from tumors. In the DOX group, the use of drugs inhibited tumor growth and reduced consumption of the body, but the side effects of DOX led to body weight reduction. Therefore, in the first 10 days after treatment, the weight of the mice in the DOX group declined. However, we also noted that at 20 days after treatment, the mice weight increased. We propose that this increase might correlate with the lost inhibition of tumor growth after the complete metabolism of DOX. This result further shows two shortcomings of DOX: the severe toxic side effects and the rapid metabolic rate. In the HNTs/DOX/LIP group, the weight of tumor-bearing nude mice was stable. Weight loss from the consumption of the body is inevitable, but this loss was much less than that in the other groups because of the enhanced antitumor effect of HNTs/DOX/LIP. The weight increase from tumor growth was less in the HNTs/DOX/LIP group than in the other groups. Thus, the weight loss resulting from drug treatment was also much less, further illustrating good biocompatibility of this drug.

Conclusion

In the present study, we generated a HNTs/DOX/LIP complex after physically mixing and package modification with soybean phospholipid. Subsequently, we verified the feasibility of DOX loading and package modification through TEM, FESEM, TGA, etc. In vitro release experiment showed that the drugs were more easily released under acidic environments like the tumor microenvironment. Moreover, we

investigated both the in vitro and in vivo antitumor efficacy and systemic toxicity of the HNTs/DOX/LIP complex as a novel anticancer drug delivery system. These results reveal that HNTs/DOX/LIP complexes more significantly inhibit tumor growth than free DOX at the same drug concentration. This enhanced antitumor efficacy of HNTs/DOX/LIP complexes is due to the effect of passively targeting the tumor region via an EPR effect as revealed by the in vivo biodistribution analysis. Moreover, we showed good biocompatibility of the HNTs/DOX/LIP complex via blood and histological examinations. Therefore, the HNT-based drug delivery system possesses good practicality as a promising platform for tumor therapy applications.

Acknowledgments

This research was financially supported by the Personnel Training Program of Shanghai Municipal Health Bureau (XBR2013082) and the Science and Technology Fund Project of Shanghai Jiao Tong University School of Medicine (16XJ21007).

Disclosure

The authors report no conflicts of interest in this work.

References

1. Jemal A, Bray F, Center MM, Ferlay J, Ward E, Forman D. Global cancer statistics. *CA Cancer J Clin*. 2011;61:69–90.
2. Jayavelu ND, Bar NS. Metabolomic studies of human gastric cancer: review. *World J Gastroenterol*. 2014;20:8092–8101.
3. Wagner AD, Grothe W, Haerting J, Kleber G, Grothey A, Fleig WE. Chemotherapy in advanced gastric cancer: a systematic review and meta-analysis based on aggregate data. *J Clin Oncol*. 2006;24:2903–2909.
4. Dai M, Yuan F, Fu C, Shen G, Hu S, Shen G. Relationship between epithelial cell adhesion molecule (EpCAM) overexpression and gastric cancer patients: a systematic review and meta-analysis. *PLoS One*. 2017;12(4):e0175357.
5. Xin Y, Huang Q, Tang J-Q, et al. Nanoscale drug delivery for targeted chemotherapy. *Cancer Lett*. 2016;379:24–31.
6. Baker K, Dunwoodie E, Jones RG, et al. Process mining routinely collected electronic health records to define real-life clinical pathways during chemotherapy. *Int J Med Inform*. 2017;103:32–41.
7. Fletcher JI, Williams RT, Henderson MJ, Norris MD, Haber M. ABC transporters as mediators of drug resistance and contributors to cancer cell biology. *Drug Resist Updat*. 2016;26:1–9.
8. Gajdacs M, Spengler G, Sanmartin C, Marc MA, Handzlik J, Dominguez-Alvarez E. Selenoesters and selenoanhydrides as novel multidrug resistance reversing agents: a confirmation study in a colon cancer MDR cell line. *Bioorg Med Chem Lett*. 2017;27:797–802.
9. Sarikaya M, Tamerler C, Jen AK, Schulten K, Baneyx F. Molecular biomimetics: nanotechnology through biology. *Nat Mater*. 2003;2:577–585.
10. Soppimath KS, Aminabhavi TM, Kulkarni AR, Rudzinski WE. Biodegradable polymeric nanoparticles as drug delivery devices. *J Control Release*. 2001;70:1–20.
11. Yu X, Trase I, Ren M, Duval K, Guo X, Chen Z. Design of nanoparticle-based carriers for targeted drug delivery. *J Nanomater*. 2016;2016:1087250.
12. Zahidah KA, Kakooei S, Ismail MC, Raja PB. Halloysite nanotubes as nanocontainer for smart coating application: a review. *Prog Org Coat*. 2017;111:175–185.
13. Oliaei E, Kaffashi B. Investigation on the properties of poly(L-lactide)/thermoplastic poly(ester urethane)/halloysite nanotube composites prepared based on prediction of halloysite nanotube location by measuring free surface energies. *Polymer*. 2016;104:104–114.
14. Handge UA, Hedicke-Hochstotter K, Altstadt V. Composites of polyamide 6 and silicate nanotubes of the mineral halloysite: influence of molecular weight on thermal, mechanical and rheological properties. *Polymer*. 2010;51:2690–2699.
15. Abdullayev E, Lvov Y. Halloysite clay nanotubes for controlled release of protective agents. *J Nanosci Nanotechnol*. 2011;11:10007–10026.
16. Viseras MT, Aguzzi C, Cerezo P, Viseras C, Valenzuela C. Equilibrium and kinetics of 5-aminosalicylic acid adsorption by halloysite. *Micropor Mesopor Mater*. 2008;108:112–116.
17. Minchinton AI, Tannock IF. Drug penetration in solid tumours. *Nat Rev Cancer*. 2006;6:583–592.
18. Octavia Y, Tocchetti CG, Gabrielson KL, Janssens S, Crijns HJ, Moens AL. Doxorubicin-induced cardiomyopathy: from molecular mechanisms to therapeutic strategies. *J Mol Cell Cardiol*. 2012;52:1213–1225.
19. Sterba M, Popelova O, Vavrova A, et al. Oxidative stress, redox signaling, and metal chelation in anthracycline cardiotoxicity and pharmacological cardioprotection. *Antioxid Redox Signal*. 2013;18:899–929.
20. Jingu K, Umezawa R, Fukui K. Radiation-induced heart disease after treatment for esophageal cancer. *Esophagus*. 2017;14:215–220.
21. Zhang Y, Xu Y, Qi Y, et al. Protective effects of dioscin against doxorubicin-induced nephrotoxicity via adjusting FXR-mediated oxidative stress and inflammation. *Toxicology*. 2017;378:53–64.
22. Wang Y, Cao XY, Guo R, et al. Targeted delivery of doxorubicin into cancer cells using a folic acid-dendrimer conjugate. *Polym Chem*. 2011;2:1754–1760.
23. Lee CC, Gillies ER, Fox ME, et al. A single dose of doxorubicin-functionalized bow-tie dendrimer cures mice bearing C-26 colon carcinomas. *Proc Natl Acad Sci U S A*. 2006;103:16649–16654.
24. Perche F, Patel NR, Torchilin VP. Accumulation and toxicity of antibody-targeted doxorubicin-loaded PEG-PE micelles in ovarian cancer cell spheroid model. *J Control Release*. 2012;164:95–102.
25. Szebeni J, Bedocs P, Urbanics R, et al. Prevention of infusion reactions to PEGylated liposomal doxorubicin via tachyphylaxis induction by placebo vesicles: a porcine model. *J Control Release*. 2012;160:382–387.
26. Yavuz MS, Cheng YY, Chen JY, et al. Gold nanocages covered by smart polymers for controlled release with near-infrared light. *Nat Mater*. 2009;8:935–939.
27. Kawamoto M, He P, Ito Y. Green processing of carbon nanomaterials. *Adv Mater*. 2017;29(25):1602423.
28. Li K, Wang SG, Wen SH, et al. Enhanced in vivo antitumor efficacy of doxorubicin encapsulated within laponite nanodisks. *ACS Appl Mater Interfaces*. 2014;6:12328–12334.
29. Diaz A, Saxena V, Gonzalez J, et al. Zirconium phosphate nanoplatelets: a novel platform for drug delivery in cancer therapy. *Chem Commun*. 2012;48:1754–1756.
30. Vergaro V, Lvov YM, Leporatti S. Halloysite clay nanotubes for resveratrol delivery to cancer cells. *Macromol Biosci*. 2012;12:1265–1271.
31. Liu Z, Sun XM, Nakayama-Ratchford N, Dai HJ. Supramolecular chemistry on water-soluble carbon nanotubes for drug loading and delivery. *ACS Nano*. 2007;1:50–56.
32. Zheng FY, Wang SG, Shen MW, Zhu MF, Shi XY. Antitumor efficacy of doxorubicin-loaded electrospun nano-hydroxyapatite-poly(lactic-co-glycolic acid) composite nanofibers. *Polym Chem*. 2013;4:933–941.
33. Qi RL, Guo R, Shen MW, et al. Electrospun poly(lactic-co-glycolic acid)/halloysite nanotube composite nanofibers for drug encapsulation and sustained release. *J Mater Chem*. 2010;20:10622–10629.
34. Deepika S, Selvaraj IC. Anticancer mechanism of unexplored plant compounds – a review. *Res J Biotechnol*. 2016;11:109–128.

35. Senchukova MA, Nikitenko NV, Tomchuk ON, Zaitsev NV, Stadnikov AA. Different types of tumor vessels in breast cancer: morphology and clinical value. *Springerplus*. 2015;4:512.
36. Goren D, Horowitz AT, Tzemach D, Tarshish M, Zalipsky S, Gabizon A. Nuclear delivery of doxorubicin via folate-targeted liposomes with bypass of multidrug-resistance efflux pump. *Clin Cancer Res*. 2000;6:1949–1957.
37. Ramzy L, Nasr M, Metwally AA, Awad GAS. Cancer nanotheranostics: a review of the role of conjugated ligands for overexpressed receptors. *Eur J Pharm Sci*. 2017;104:273–292.
38. Wang C, Tao HQ, Cheng L, Liu Z. Near-infrared light induced in vivo photodynamic therapy of cancer based on upconversion nanoparticles. *Biomaterials*. 2011;32:6145–6154.